JOURNAL OF SPACECRAFT AND ROCKETS
Vol. 33, No. 2, March–April 1996

Parametric and Classical Resonance in Passive Satellite Aerostabilization

Renjith R. Kumar,* Daniel D. Mazanek,† and Michael L. Heck*
Analytical Mechanics Associates, Inc., Hampton, Virginia 23666-1398

Purely passive aerostabilization of satellites has never been flight demonstrated. The Shuttle hitchhiker passive aerodynamically stabilized magnetically damped satellite experiment would be the first flight experiment of its kind that, in conjunction with results from a high-fidelity computer simulator, would corroborate attitude stability. Pure aerostabilization, with no gravity gradient restoring torques, if proved, is highly desirable for future missions such as the gravity and magnetic Earth surveyor. High-fidelity nonlinear simulation results indicate interesting attitude behavior, such as cone angle transients that provoke the need for sound theoretical justification. A wind vane in a wind field model is used to derive simple analogous Mathieu–Hill equations of motion, the stability properties of which are predicted via Floquet theory. Parametric resonance caused by higher order of the once per orbit density harmonics, varying natural frequency of oscillation as a result of altitude decay, and varying wind magnitude due to global winds are studied in detail. The simple time-varying linear wind vane analogy captures the essence of the observations made with the complex nonlinear simulation. Classical resonance because of step changes in the solar torques as a result of Earth occultation is also discussed. Based on insight obtained from the stability properties observed for the wind vane analogy, an optimal satellite is designed that provides best attitude performance while maintaining sufficient lifetime and other mission constraints.

Nomenclature

A = area of analogous wind vane, m^2
B = average ballistic coefficient of subsat, kg/m^2
I = moment of inertia about an axis of rotation, kg-m^2
K = aerodynamic moment stiffness, N-m/rad
l_b = length of back shell, cm
l_f = length of front shell, cm
M = mass of subsat, kg
r = center-of-pressure to center-of-mass offset, m
r_i = inner radius of front shell, cm
T_{aero} = aerodynamic torque, N-m
t_b = thickness of back shell, cm
t_f = thickness of front shell, cm
V = velocity magnitude of wind, m/s
β = cone angle of the satellite, rad
Δ = damping ratio
ε = coefficient of damping, N-m-s/rad
θ = angle of rotation of wind vane from reference wind direction, rad
ϱ = density of air, kg/m^3
ϱ_{amp} = amplitude of once/orbit harmonic of ϱ, kg/m^3
ϱ_b = density of back shell, kg/m^3
ϱ_{bias} = bias component of density of air profile over one orbit, kg/m^3
ϱ_f = density of front shell, kg/m^3
σ_D, σ_B = accommodation coefficients
Ω = natural frequency of oscillation of wind vane, rad/s
ω = once per orbit frequency, rad/s

Introduction

A PASSIVE aerodynamically stabilized magnetically damped subsatellite (subsat) was envisioned by NASA Goddard Space Flight Center (GSFC) engineers as a low-cost, low-weight, long lifetime option for the gravity and magnetic Earth surveyor (GAMES) mission.[1] The subsat, which has inertial properties of a uniform sphere, is completely passive and carries a corner cube retroreflector[2] on its front face that reflects a laser beam projected on it by an active main satellite. The main satellite performs station keeping with respect to the subsat at a distance of 200 km (±50 km) in a nearly circular orbit of altitude varying from 325 to 250 km due to drag decay. A mission requirement imposed on the subsat attitude performance is that the cone angle, defined as the angle between the orbital velocity vector and the subsat body X axis, as shown in Fig. 1, is small. This requirement is to ensure good return strength of the reflected laser beam. Ideally, the steady-state cone angle should be less than 9 deg subject to all other mission constraints being satisfied. No restriction is imposed on the roll angle of the spacecraft. Note that there exists no gravity gradient restoring torques acting on the satellite owing to its mass distribution.

The attitude performance of an aerostabilized magnetically damped satellite is currently being simulated at NASA Langley Research Center, using high-fidelity models[3] of aerodynamic torques, including global wind effects, solar radiation torques, magnetic damping torques, and realistic orbital dynamics. Moreover, the Shuttle hitchhiker passive aerodynamically stabilized magnetically damped satellite (PAMS) experiment,[1] to be flown in early 1996, will be used to validate aerodynamic stability and magnetic hysteresis damping.[4]

This paper provides a complete understanding of the stability properties of a generic aerodynamically stabilized magnetically

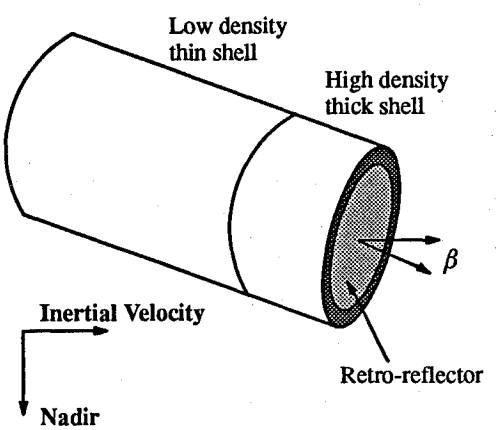

Fig. 1 GAMES subsat schematic.

Received Dec. 16, 1994; revision received Sept. 20, 1995; accepted for publication Oct. 13, 1995.

*Senior Engineer. Member AIAA.
†Senior Project Engineer.

damped satellite attitude dynamics that is required to explain and corroborate results from the high-fidelity nonlinear simulator and to help suggest design modifications for the experimental PAMS and the GAMES subsat. The analysis was conducted over several phases: 1) only aerodynamic torques with the effect of altitude decay, 2) effect of passive damping, 3) solar radiation effects, and 4) effect of global winds.

Discussion

Aerodynamic Restoring Torques and Effect of Altitude Decay

The pitch and yaw attitude dynamics of the subsat can be uncoupled and each channel treated as analogous wind vanes in a wind field. Since the disturbing rotating atmosphere and the horizontal global winds are primary in the yaw channel, the simplified yaw dynamics are considered. The wind field can be assumed to be in a constant direction (as in an equatorial orbit) or oscillating (because of rotating atmosphere effects in higher inclinations). For the former case, it can be shown that the wind vane dynamics, for small angles, imitate a simple mass-spring system as

$$I\ddot{\theta} = T_{\text{aero}} = -K(t,\theta)\theta \tag{1}$$

The aerodynamic torque can be written as the product of aerodynamic moment stiffness and the rotation angle. The aerodynamic moment stiffness is a function of the rotation angle and time. As seen in Fig. 2, the aerodynamic torque varies nonlinearly with θ. For a given small range of θ, say, from zero to 10 deg, however, the aerodynamic torque can be assumed to be a linear function of θ. In Fig. 2, the abscissa is either pitch or yaw angle (because of longitudinal symmetry) of the satellite with respect to the wind, and the ordinate is the normalized aerodynamic torque along the respective axis. Normalization is performed with respect to the dynamic pressure. The graph is obtained for specific values of the aerodynamic accommodation coefficients,[3] σ_D and σ_B. The aerodynamic roll torque is zero. It can be easily shown that the stiffness term is proportional to the density of the incoming wind, the area of the vane, the square of the velocity of the wind, and the center-of-pressure (CP) to center-of-mass (CM) offset. The time-varying density profile results from decaying altitude, diurnal bulge effect, and other atmospheric effects.[5] Thus,

$$K(t) \propto \varrho(t)V^2Ar \tag{2}$$

or, introducing a constant of proportionality c,

$$K(t) = c\,\varrho(t)V^2Ar \tag{3}$$

Ignoring the slowly changing exponential increase in density because of altitude decay, the density profile contains at least a bias

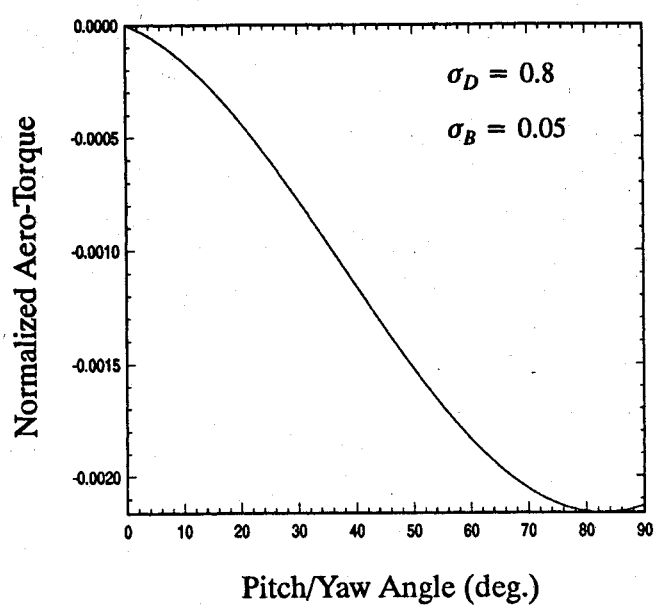

Fig. 2 Normalized aerodynamic torque vs pitch/yaw angle.

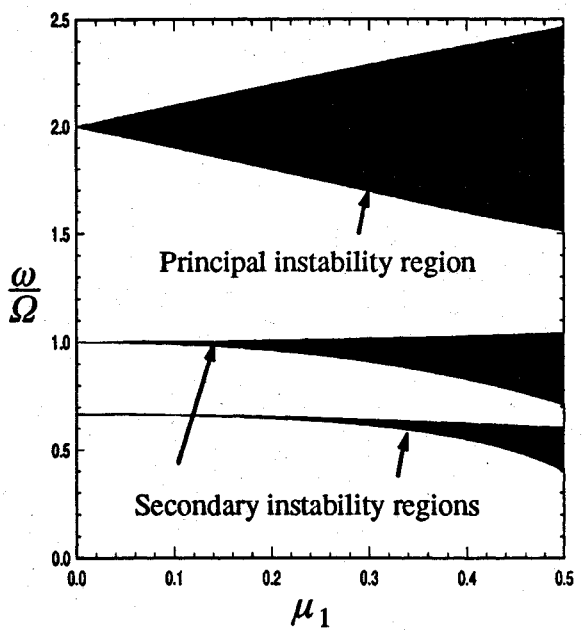

Fig. 3 First three major instability regions of Mathieu equation.

term and a once per orbit frequency sinusoidal term because of the diurnal bulge effect, i.e.,

$$\varrho(t) = \varrho_{\text{bias}} + \varrho_{\text{amp}} \cos \omega t \tag{4}$$

Thus, Eq. (1) can be approximated by the following equation:

$$\ddot{\theta} + \Omega^2[1 + 2\mu_1 \cos \omega t]\theta = 0 \tag{5}$$

where

$$\Omega = \sqrt{\frac{cAV^2r\varrho_{\text{bias}}}{I}} \tag{6}$$

denotes the natural frequency of oscillation and μ_1 is defined by $2\mu_1 = \varrho_{\text{amp}}/\varrho_{\text{bias}}$. Note that the natural frequency slowly increases because of increasing bias density as altitude decays because of drag. Equation (5) is known as the Mathieu equation, commonly arising in dynamics of elastic systems. Floquet theory and infinite determinant evaluation schemes[6] are used to characterize the stability properties of the Mathieu equation. Figure 3 depicts the major instability regions of the system given by Eq. (5) as a function of μ_1 and ω/Ω.

Figure 4 shows the cone angle time-history results of the nonlinear simulation of a GAMES subsat in an equatorial orbit, assuming a density profile as in Eq. (4) and assuming that ϱ_{bias} and ϱ_{amp} increase as altitude decays. The cone angle profile shows no transients [transients indicate passing through instability regions in the $\mu_1 - (\omega/\Omega)$ stability diagram]. This is because the principal instability region for $\mu_1 \to 0$ occurs at $\omega/\Omega = 2/1$, and for the nominal GAMES mission design, $\omega/\Omega < 1/5$. Thus, no principal instability regions are crossed as Ω increases. For $\mu_1 \to 0$, the secondary regions of instability that occur at $\omega/\Omega = 2/2, 2/3, 2/4, \ldots$, are thin regions and hence, instability or parametric resonance that occurs as ω/Ω crosses values of $2/10, 2/11, 2/12, \ldots$, persists only for a very short duration of time. Also note that the peak cone angle reduces, as seen in Fig. 4, and the frequency of oscillation increases as the stiffness increases.

A realistic sample density profile calculated assuming a Jacchia 70 atmosphere[5] and its fast Fourier transform (FFT) for a nominal GAMES inclination of 87 deg are shown in Figs. 5 and 6, respectively. The FFT indicates that the density profile has not only the bias and once per orbit frequencies, but higher harmonics of orbit frequency as well. The Mathieu equation cannot directly be used to analyze this system. A generalization of the Mathieu equation

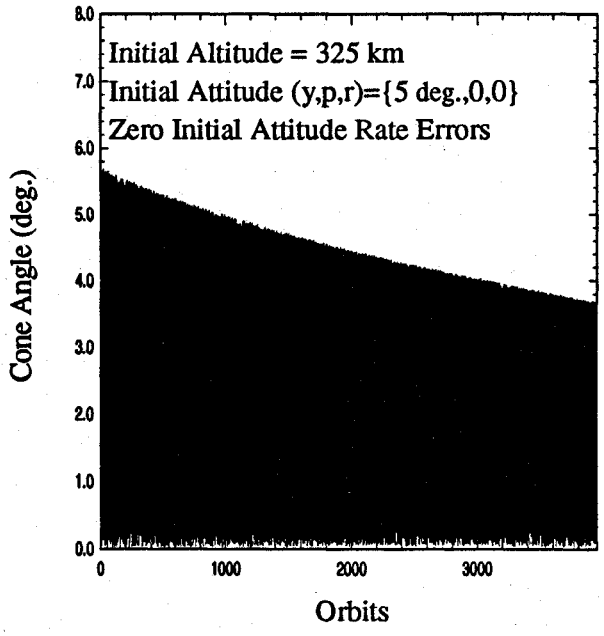

Fig. 4 Cone angle profile in an equatorial orbit.

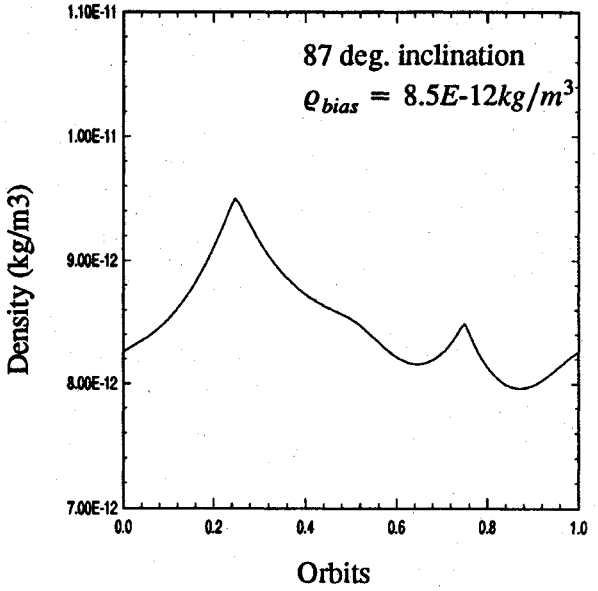

Fig. 5 Typical density profile.

referred to as the Hill equation[6] is used to completely characterize the stability and instability regions. The Hill equation is given by

$$\ddot{\theta} + \Omega^2 \left[1 + 2 \sum_{i=1}^{i=\infty} \mu_i \cos i\omega t \right] \theta = 0 \qquad (7)$$

Stability analysis of the Hill equation is performed by assuming $\mu_1 = 0, i \neq 1$, and performing stability analysis on the resulting Mathieu equation and continuing this procedure for all values of i, where $\mu_i \neq 0$. To a first-order approximation,[6] the resulting stability diagram is a superimposition of the multiple Mathieu stability diagrams for all values of nonzero μ_i. The following paragraphs show that the secondary regions of instability of the Mathieu equation become principal regions of stability of the Hill equation for corresponding values of nonzero μ_i.

Let $\mu_i = 0$, $i \neq 1$, and $\mu_1 \to 0$. Then from the stability analysis of the Mathieu equation it is clear that instability occurs at $\omega/\Omega = 2^*/1, 2/2, 2/3, 2/4, \ldots$. Here the superscript * denotes principal instability region. Now let $\mu_i = 0, i \neq 2$, and $\mu_2 \to 0$. Then from the stability analysis of the Mathieu equation with ω replaced by 2ω, instability occurs when $2\omega/\Omega = 2^*/1, 2/2, 2/3, 2/4, \ldots$,

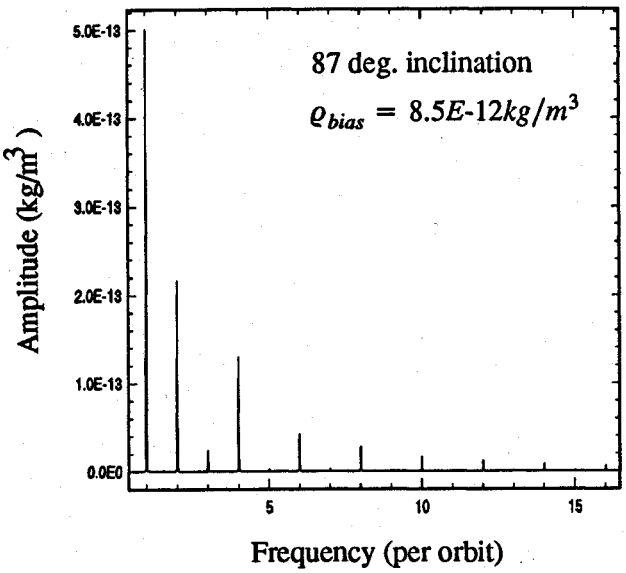

Fig. 6 FFT of density profile.

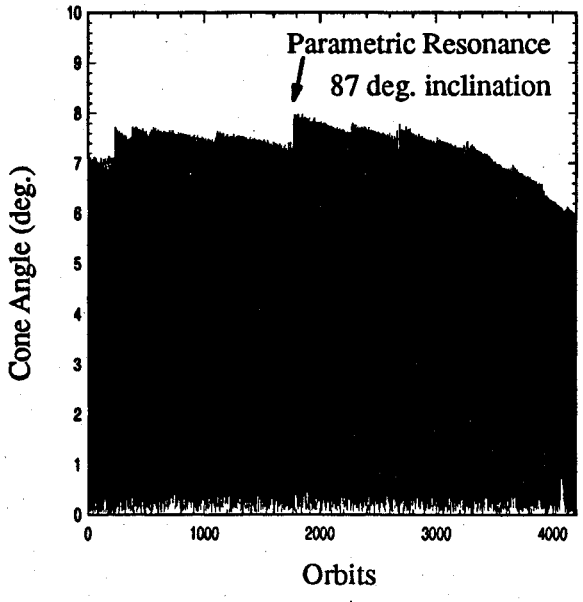

Fig. 7 Cone angle profile of nominal subsat.

which implies that instability occurs at $\omega/\Omega = 2^*/2, 2/4, 2/6, 2/8, \ldots$. Similarly, for $\mu_i = 0$, $i \neq 3$, and $\mu_3 \to 0$, instability occurs when $3\omega/\Omega = 2^*/1, 2/2, 2/3, 2/4, \ldots$, or equivalently at $\omega/\Omega = 2^*/3, 2/6, 2/9, 2/12, \ldots$. Thus the secondary regions of instability of the Mathieu equation, i.e., $\omega/\Omega = 2/2, 2/3, 2/4, \ldots$, become principal regions of instability of the Hill equation, provided the corresponding $\mu_i \neq 0$. Note that, in general, the magnitude of μ_i reduces as i increases.

Figure 7 shows the cone angle time history of a nominal GAMES subsat in an 87-deg inclination orbit. The initial yaw angle chosen was 7 deg (close to the peak yaw angle that would result for an undamped aerostabilized satellite from rotating atmosphere effects at 87-deg inclination) and the initial attitude rate errors were zero. Rotating atmosphere effects were neglected. The transients in the cone angle performance can be precisely correlated to the crossing of the ω/Ω ratio through $2/10, 2/11, 2/12, \ldots$, which are now principal instability regions for the nonzero μ_i, $i = 10, 11, 12, \ldots$, as seen in Fig. 6. The addition of rotating atmosphere does not change secular trends in the cone angle profile. Thus, the simple linear time-varying analogous Mathieu–Hill equations can be used to clearly explain the anomalies (transients) observed in the cone angle output of the nonlinear simulation.

A decrease in the inertia increases the natural frequency that causes ω/Ω to cross principal instability regions for smaller ratios

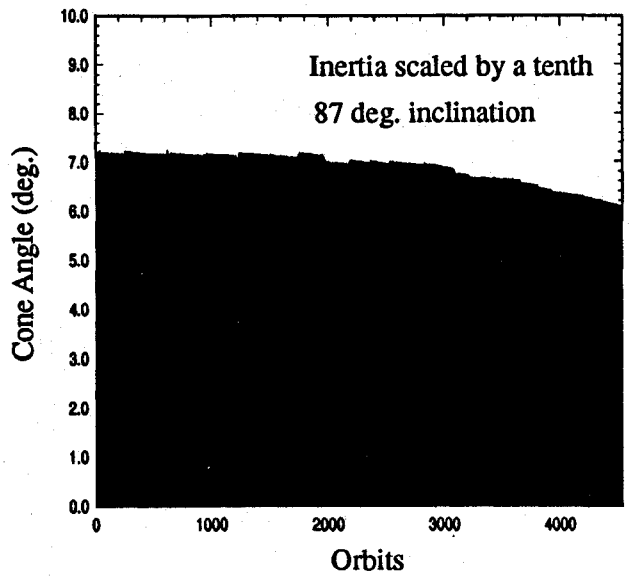

Fig. 8 Cone angle profile of modified subsat.

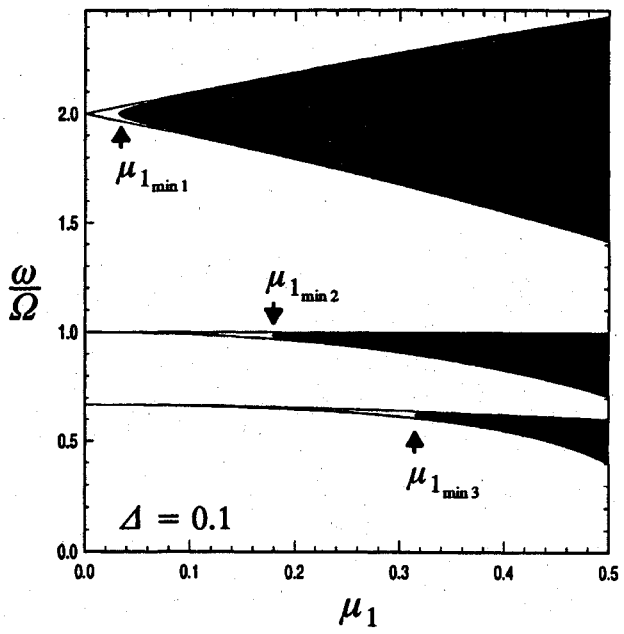

Fig. 9 Instability regions with damping.

that have smaller associated magnitudes for μ_i. Hence, the transients should be smaller. This is verified by simulating a modified GAMES subsat with 1/10 the inertia as shown in Fig. 8. From a design viewpoint, note that although decreasing inertia reduces the adverse effects of parametric resonance, it also maps into decreased mass of the satellite, for given volume constraints. This decreased mass reduces ballistic coefficient and hence orbital lifetime. Similarly, increasing the CP–CM offset, area, and density also increase natural frequency, but adversely impact lifetime. Although increasing CP–CM offset does not directly cause lower ballistic coefficient, a GAMES mission constraint that the corner cube retroreflector vertex be at the center of mass of the satellite[3] implies a longer satellite and hence larger drag for nonzero cone angle attitudes.

Effect of Passive Damping

In this phase of the study, the effect of damping on the aerostabilized satellite is addressed. The damped Mathieu equation (8) is used to derive the stability and instability regions:

$$\ddot{\theta} = 2\varepsilon\dot{\theta} + \Omega^2[1 + 2\mu_1 \cos \omega t]\theta = 0 \tag{8}$$

where

$$\varepsilon = \Delta\Omega/2\pi \tag{9}$$

As Δ is increased, the minimum value of μ_1 to cause instability also increases.[6] It has been shown[6] that this minimum value can be approximated by

$$\mu_{1_{\min_j}} = \sqrt[j]{\Delta/\pi} \tag{10}$$

where j denotes the index on the instability region, i.e., $j = 1$ for principal instability, etc. Figure 9 denotes the stability and instability regions in the $\mu_1 - (\omega/\Omega)$ parameter space. Note that $\mu_{1_{\min_1}}$ increases linearly with Δ, and $\mu_{1_{\min_2}}$ increases with the square root of Δ, and so on.

Thus, if a pure rate-damping device could be employed for the aerostabilized satellite, then there exists a Δ, or equivalently ε, that could prevent parametric resonance. A feasible, off-the-shelf, pure rate-damping device does not exist for the GAMES subsat. The damping device proposed for GAMES subsat and PAMS are magnetic hysteresis rods.

The magnetic hysteresis damping introduces additional attitude-dependant perturbation terms resulting from interactions with the Earth's geomagnetic field (unlike pure rate damping which has only the $2\varepsilon\dot{\theta}$ term). One of the terms takes the form $\Omega^2[2\nu_2 \cos 2\omega t]\theta$, where ν_2 is a constant. This term when added to Eq. (8) resembles a damped Hill equation with $\mu_2 = \nu_2$. Whereas for pure rate damping, increasing Δ, increases $\mu_{1_{\min_j}}$ and thus ameliorates parametric resonance, the additional stiffness term introduced by magnetic hysteresis damping could actually worsen parametric resonance as explained next.

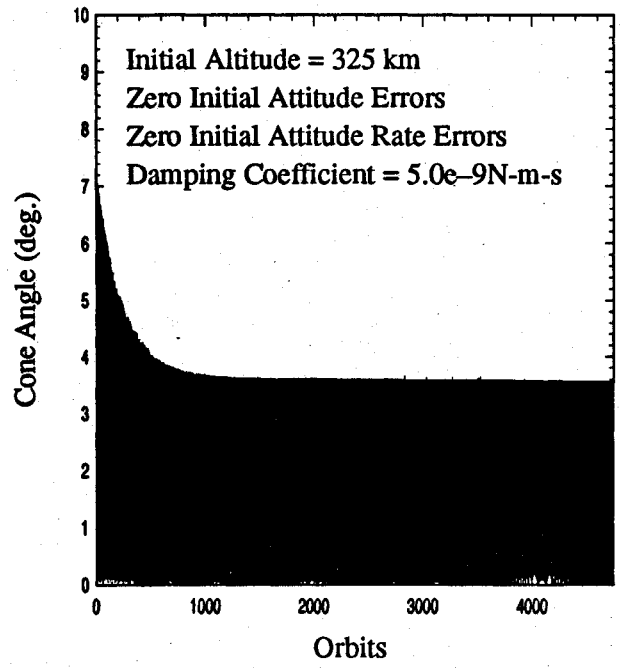

Fig. 10 GAMES subsat cone angle profile with pure rate damping.

As damping is increased, $\mu_{2_{\min_j}}$ also increases in the same fashion as shown in Eq. (10). Thus the instability region moves toward the right. However, ν_2 increases linearly with Δ, and since $\mu_2 = \nu_2$, the location in the $\mu_2 - (\omega/\Omega)$ diagram also moves to the right. For the principal instability region in the $\mu_2 - (\omega/\Omega)$ diagram, μ_2 and $\mu_{2_{\min_1}}$ move to the right proportionally, whereas for the secondary regions of instability, μ_2 moves much faster to the right than $\mu_{2_{\min_j}}$, $j \neq 1$.

Figure 10 depicts the cone angle profile of a nominal GAMES subsat simulation in an 87-deg inclination orbit. For academic purposes, a hypothetical pure rate damper was used as the damping device. The steady-state peak cone angle is only 3.6 deg, which corresponds to the maximum deviation of the resultant velocity vector from the local horizontal resulting from rotating atmosphere effects. No parametric resonance is observed. On the other hand, the cone angle profile resulting from a similar simulation with the pure

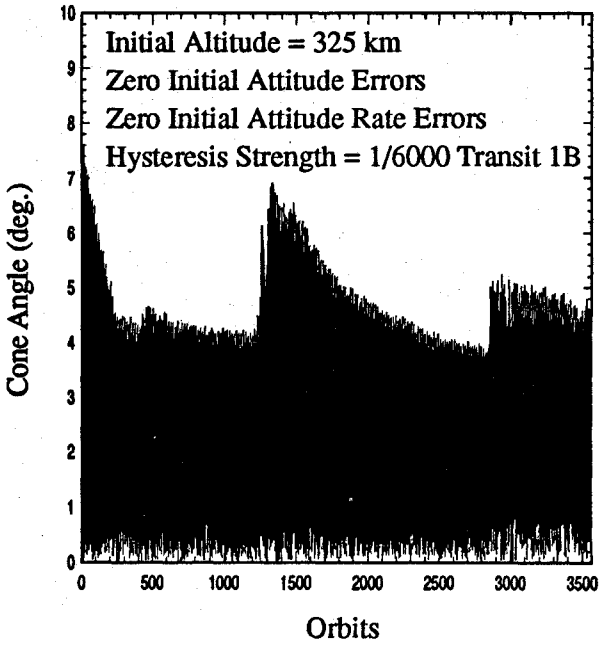

Fig. 11 GAMES subsat cone angle profile with magnetic hysteresis damping.

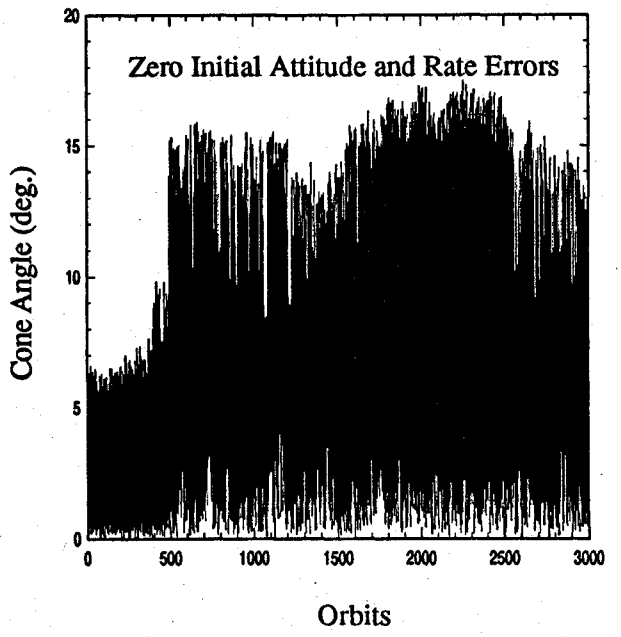

Fig. 12 Effect of solar radiation (Earth occultation on).

rate damper replaced by the magnetic hysteresis damping device is shown in Fig. 11. Note the large transients because of parametric resonance.

Solar Radiation Effects

The solar radiation torque is an external disturbance approximately one to two orders of magnitude smaller (for a nominal GAMES configuration) than the aerodynamic restoring torques below 325-km altitude. Because of the satellite going in and out of Earth occultation, however, the solar torque time history is in the form of step functions. It is well known that a step function has energy at all frequencies, with most of the energy content at lower frequencies. The energy content of the step function at the natural frequency of oscillation of the satellite causes classical resonance in the absence of damping. The cone angle profile of an undamped GAMES simulation in a 325-km circular orbit with rotating atmosphere and solar radiation torques is shown in Fig. 12.

Artificially removing Earth's occultation prevents resonance in the presence of solar radiation torques as shown in Fig. 13.

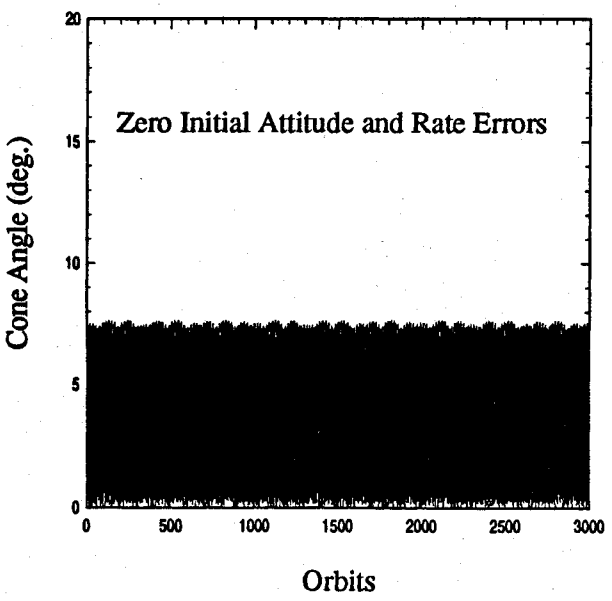

Fig. 13 Effect of solar radiation (no Earth occultation).

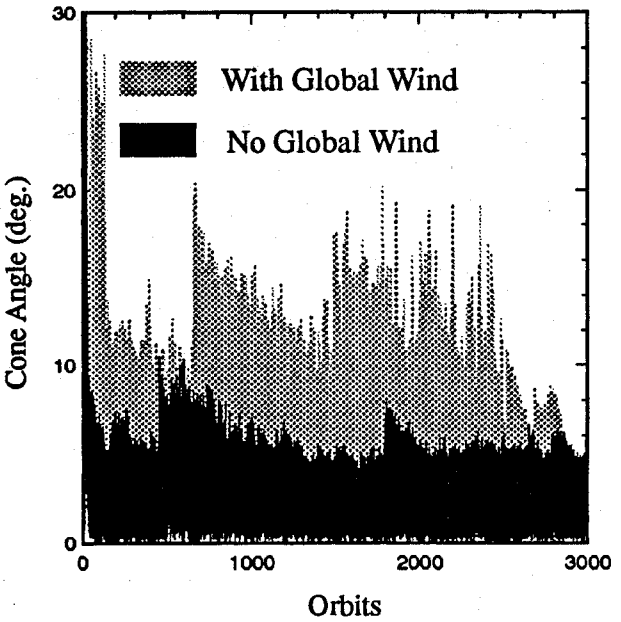

Fig. 14 Simulation results with and without global winds.

Moreover, it was observed that an attitude independent zero mean square wave solar torque (test signal) causes resonance and instability in the aerostabilized satellite cone angle, whereas a zero mean sinusoidal solar torque introduces no resonance.

Thus, it can be concluded that the step changes in solar torques have a tendency to destabilize the aerostabilized satellite in the absence of damping. Note that the nonlinear simulation does not model the penumbra to umbra transition. At orbital velocities in the order of 7 km/s, however, the transition is so fast that the solar torque near the terminator mimics a step function.

Effect of Global Winds

The global winds[3] are wind patterns primarily in the horizontal plane. The wind magnitude is larger at higher latitudes. Polar storms can have wind magnitudes of 600 m/s. These global winds introduce additional terms in the Hill equation. The natural frequency of oscillation varies (by $\pm 5\%$) even in the absence of altitude decay, because of the varying magnitude and direction of the winds. Hence, parametric resonance can occur even in the absence of altitude decay. Apart from parametric resonance, the global winds also cause the peak cone angle to increase because of larger variations of the resultant velocity vector from the local horizontal. Figure 14 compares a

nominal GAMES simulation result with and without global winds. Nominal[3] implies the presence of rotating atmosphere effects, solar torques, and nominal damping.

Nominal GAMES Subsat Design

The original GAMES subsat configuration designed by NASA GSFC had a mass distribution such that all three moments of inertia were equal. This prevented any gravity gradient torques. The center of mass of the satellite was at the vertex of the corner cube to prevent any velocity error contribution to the laser-ranging data because of rotational rates of the subsat. The ballistic coefficient was high enough to provide the desired 6-month lifetime and the mass was approximately 4.5 kg. Figure 15 depicts the side view of the GAMES subsat with the original design values of the seven parameters obtained from GSFC.

Magnetic hysteresis rod strengths were chosen (three orthogonal rods along each of the body axes with 1/6000th the volume of TRANSIT 1B rod[4]) such that an acceptable damping time of less than 1 week was obtained for worst-case deployment rate errors anticipated, i.e., 0.5 deg/s/axis. Higher strengths of hysteresis rods provides quicker damping, but introduces larger steady-state pointing errors, since hysteresis torques are perturbing torques once steady state is achieved. Figure 16 depicts the cone angle performance of a nominal GAMES simulation. The initial orbit is 325-km circular at an inclination of 87 deg and an arbitrary initial ascending node of −45 deg. The simulation is stopped at an altitude of 250 km. Initial attitude was assumed to be local vertical local horizontal, but the initial attitude rate errors were 0.5 deg/s/axis. Nominal simulation implies statistical mean values of flux and geomagnetic index for the nominal mission timing with launch data April 1, 1998. The

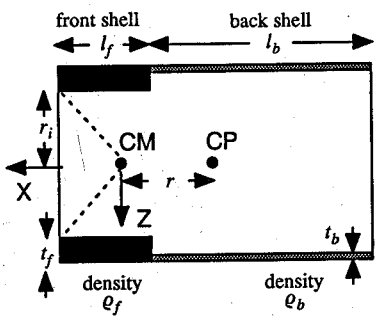

Fig. 15 Nominal GAMES subsat design. r_i = 3.0 cm, t_f = 1.32 cm, t_b = 0.0787 cm, l_f = 8.13 cm, l_b = 11.68 cm, ϱ_f = 18,827 kg /m^3 (depleted uranium), and ϱ_b = 2710 kg/m^3 (aluminum).

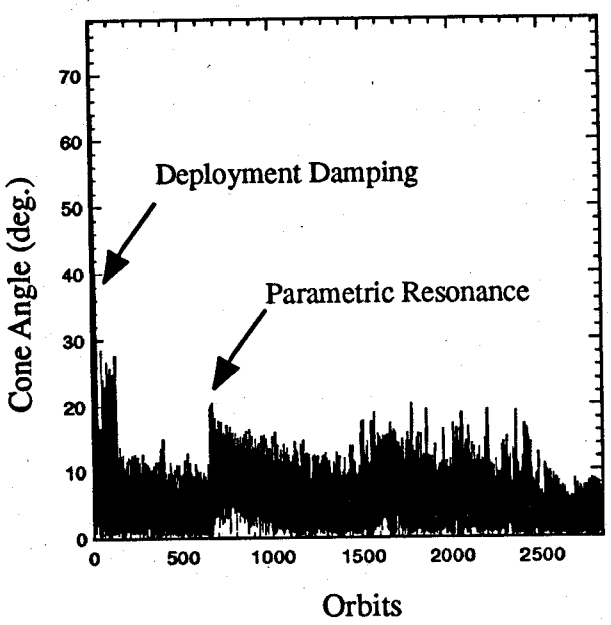

Fig. 16 Nominal GAMES simulation result.

nominal values of the accommodation coefficients are midpoints of the possible range of the coefficient.[3] Statistical mean global winds are also simulated.

Design Recommendation

The four-phase study characterized aerostabilization and passive damping and provided insight into satellite attitude behavior in the presence of external disturbances, such as solar radiation torques and global winds. Variables that affect attitude performance are the density of the incoming wind, the analogous wind vane area, the velocity of the wind, and the CP–CM offset. Of the preceding, the density and velocity are not design parameters. The natural frequency is given by Eq. (6).

Increasing the natural frequency reduces the adverse effects of parametric resonance. Increasing the natural frequency increases the aerodynamic restoring torque per unit inertia, but also increases the global wind disturbance torques per unit inertia. Increasing r, A, and/or decreasing I to move the natural frequency to a higher value in an attempt to utilize lower energy of the solar step function at higher frequency is futile since the solar torque per unit inertia itself increases. Reducing solar CP–CM offset via carefully designed surface coatings, and reducing occultation via launch date dependant sun-synchronous orbits are design and mission modifications worth consideration. Decreasing inertia maps to lower mass that implies a bigger mass budget for GAMES main satellite, but shortens lifetime due to lower ballistic coefficient. Thus, one can easily infer that increasing the natural frequency has both merits and disadvantages. For the GAMES mission, it has been observed that increasing the natural frequency improves cone angle performance and the tradeoff is lifetime. However, this cannot be generalized for an arbitrary aerostabilized satellite and mission.

Optimal Design

The following constrained parameter optimization problem was posed and solved to design an optimal subsat. The design parameter bounds are given in Eqs. (11–17) and the other mission constraints are captured in Eqs. (18–21). The optimization problem is

$$\text{Maximize} \qquad r/I$$

subject to parameter bounds

$$3 \le r_i \le 10 \tag{11}$$

$$0 \le l_f \le 50 \tag{12}$$

$$0 \le l_b \le 50 \tag{13}$$

$$0.05 \le t_f \le 5 \tag{14}$$

$$0.05 \le t_b \le 5 \tag{15}$$

$$2710 \le \varrho_f \le 19{,}300 \tag{16}$$

$$2710 \le \varrho_b \le 19{,}300 \tag{17}$$

and subject to constraints

$$\text{CM at vertex of retroreflector} \tag{18}$$

$$0 \le M \le 8 \tag{19}$$

$$350 \le B \le 500 \tag{20}$$

$$-10\% \le \frac{(I_x - I_y)100}{I_x} \le +10\% \tag{21}$$

The objective function chosen is a measure of the natural frequency. Since the dynamic pressure is not a design variable and since a larger CP–CM automatically implies a larger area, the ratio r/I is chosen as the measure of natural frequency. Here I was chosen to be inertia along the yaw channel, i.e., I_z (same as I_y) and the inertia of the corner cube was ignored. The minimum radius of the corner cube r_i required for sufficient strength of return laser signal was prescribed as 3 cm. A study on inertia imperfections resulting

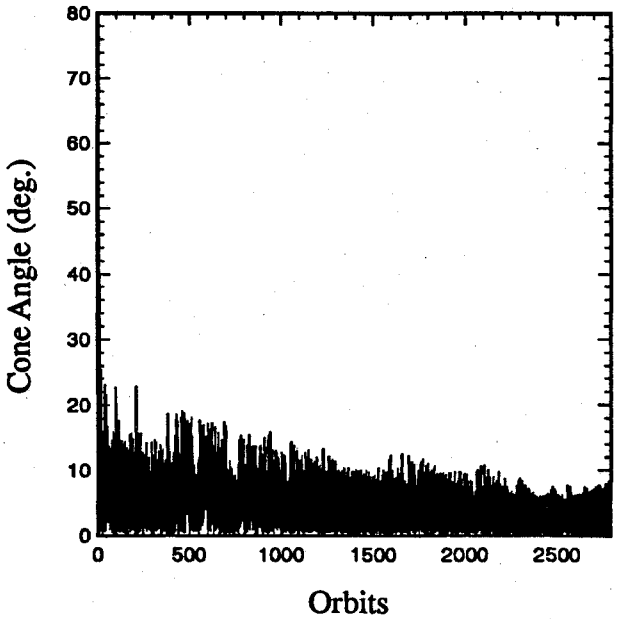

Fig. 17 Optimized GAMES simulation result.

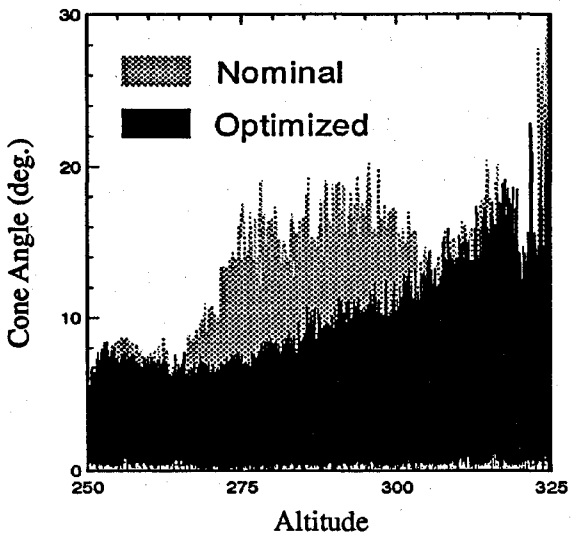

Fig. 18 Comparison of optimized vs nominal GAMES cone angle.

from manufacturing errors indicated that a ±10% error in inertia (mapped into gravity gradient stiffness) had no substantial effect on the cone angle performance. Thus the last constraint is bounded by ±10%, instead of 0%. The optimization was performed by using an industry standard nonlinear constrained optimization software NPSOL.[7] The design parameters obtained from the constrained optimization solution are as follows: $r_i = 3.0$ cm, $t_f = 1.272$ cm, $t_b = 0.05$ cm, $l_f = 8.112$ cm, $l_b = 18.151$ cm, $\varrho_f = 19{,}300$ kg/m^3(gold), and $\varrho_b = 2710$ kg/m^3 (aluminum).

A nominal simulation of the optimized GAMES subsat is shown in Fig. 17. Note that the transients resulting from parametric resonance have been reduced considerably compared to Fig. 16. The lifetime is approximately 6 months. Figure 18 compares the cone angle performance of the nominal and optimized GAMES subsat. Altitude, varying from 325 to 250 km, is chosen as the X axis. The improvement in performance of the optimized GAMES subsat can be seen, especially at lower altitudes. The smaller the cone angle, the better is the resulting signal returned from the subsat.

Conclusions

A simple wind vane dynamics in a wind field was used as an analogy to study the yaw dynamics (most significant) of an aerostabilized satellite. The resulting Mathieu–Hill equations were used to characterize parametric resonance. Parametric resonance caused by higher order of the once per orbit density harmonics, varying natural frequency of oscillation because of altitude decay, and varying wind magnitude because of global winds were precisely correlated to the crossing of the theoretically predicted instability regions of the Mathieu–Hill equations.

It is shown that pure rate-damping devices can ameliorate parametric resonance. Magnetic hysteresis rods, however, introduce stiffness-like terms in addition to pure damping in the analogous damped Mathieu–Hill equations that could adversely affect parametric resonance.

The Earth occultation causes step changes in the solar radiation torque that contains frequencies that span the entire spectrum. Such a forcing function causes classical resonance in the aerostabilized subsat in the absence of damping.

The global winds, with varying wind magnitudes and direction, changes the natural frequency of oscillation by ±5%. Thus parametric resonance could occur even in the absence of altitude decay. Moreover, the widely changing wind direction can cause the peak cone angle to increase substantially.

In general, increasing the natural frequency of oscillation of an aerostabilized satellite has both merits and disadvantages with respect to attitude performance. For the GAMES mission, increasing the natural frequency improves cone angle performance and the tradeoff is lifetime. Hence, a simple constrained optimization problem was posed and solved to obtain an optimum GAMES subsat.

Acknowledgments

This work was completed under Contract NAS1-18935 with Space Systems and Concepts Division at NASA Langley Research Center. The authors would like to acknowledge the support of James W. Johnson, Technical Monitor.

References

[1]Pacini, L., and Skillman, D., "A Passive Aerodynamically Stabilized Satellite for Low Earth Orbit," AAS/AIAA Paper 95-173, Feb. 1995.

[2]Ruck, G. T., Barrick, D. E., Stewart, W. D., and Krishbaum, C. K., *Radar Cross Section Handbook*, Plenum, New York, 1970, pp. 588–596.

[3]Kumar, R. R., Mazanek, D. D., and Heck, M. L., "Simulation and Shuttle Hitchhiker Validation of Passive Satellite Aero-Stabilization," *Journal of Spacecraft and Rockets*, Vol. 32, No. 5, 1995, pp. 806–811.

[4]Fischell, R. E., "Magnetic Damping of the Angular Motions of Earth Satellites," *ARS Journal*, Vol. 31, No. 9, 1961, pp. 1210–1217.

[5]Jacchia, L. G., "New Static Models of the Thermosphere and Exosphere with Emperical Temperature Profiles," Smithsonian Astrophysical Observatory Special Rept. 313, 1970.

[6]Bolotin, V. V., *The Dynamic Stability of Elastic Systems*, Holden–Day Series in Mathematical Physics, Holden–Day, San Francisco, 1964.

[7]Gill, P. E., Murray, W., Saunders, M. A., and Wright, M. H., "User's Guide for NPSOL: A Fortran Package for Nonlinear Programming," Dept. of Operations Research, TR SOL86-2, Stanford Univ., Stanford, CA, Jan. 1986.

E. A. Thornton
Associate Editor